

Dynamics of uniaxial hard ellipsoids.

Cristiano De Michele,¹ Rolf Schilling,² and Francesco Sciortino¹

¹*Dipartimento di Fisica and INFM-CRS Soft,*

Università di Roma La Sapienza, P.le A. Moro 2, 00185 Roma, Italy

²*Johannes-Gutenberg-Universitat Mainz, D-55099 Mainz, Germany*

(Dated: February 1, 2008)

Abstract

We study the dynamics of monodisperse hard ellipsoids via a new event-driven molecular dynamics algorithm as a function of volume fraction ϕ and aspect ratio X_0 . We evaluate the translational D_{trans} and the rotational D_{rot} diffusion coefficient and the associated isodiffusivity lines in the $\phi - X_0$ plane. We observe a decoupling of the translational and rotational dynamics which generates an almost perpendicular crossing of the D_{trans} and D_{rot} isodiffusivity lines. While the self intermediate scattering function exhibits stretched relaxation, i.e. glassy dynamics, only for large ϕ and $X_0 \approx 1$, the second order orientational correlator $C_2(t)$ shows stretching only for large and small X_0 values. We discuss these findings in the context of a possible pre-nematic order driven glass transition.

PACS numbers: 64.70.Pf, 61.20.Ja, 61.25.Em, 61.20.Lc

Particles interacting with only excluded volume interaction may exhibit a rich phase diagram, despite the absence of any attraction. Spherical objects, in equilibrium, present only a fluid and a crystal phase, while simple non-spherical hard-core particles can form either crystalline or liquid crystalline ordered phases[1], as first shown analytically by Onsager[2] for rod-like particles. Successive works have established detailed phase diagrams for several hard-body shapes[3, 4, 5, 6] and have clarified the role of the entropy in the transition between different phases. Less detailed information are available concerning dynamic properties of hard-core bodies and their kinetically arrested states. In the case of the hard-sphere system, dynamics slows down significantly on increasing packing fraction ϕ , and, when crystallization is avoided (mostly due to intrinsic sample polydispersity), a dynamic arrested state (a glass) with extremely long life time can be generated. The slowing down of the dynamics is well described by mode coupling theory (MCT)[7]. On going from spheres to non-spherical particles, non-trivial phenomena arise, due to the interplay between translational and rotational degrees of freedom. The slowing down of the dynamics can indeed appear either in both translational and rotational properties or in just one of the two.

Hard ellipsoids (HE) of revolution [1, 8] are one of the most prominent systems composed by hard body anisotropic particles. HE are characterized by the aspect ratio $X_0 = a/b$ (where a is the length of the revolution axis, b of the two others) and by the packing fraction $\phi = \pi X_0 b^3 N / 6V$, where N is the number of particles and V the volume. The equilibrium phase diagram, evaluated numerically two decades ago [9], shows an isotropic fluid phase (I) and several ordered phases (plastic solid, solid, nematic N). The coexistence lines show a swallow-like dependence with a minimum at the spherical limit $X_0 = 1$ and a maximum at $X_0 \approx 0.5$ and $X_0 \approx 2$ (cf. Figure 1). Application to HE[10] of the molecular MCT (MMCT)[11, 12] predicts also a swallow-like glass transition line. In addition, the theory suggests that for $X_0 \lesssim 0.5$ and $X_0 \gtrsim 2$, the glass transition is driven by a precursor of nematic order, resulting in an orientational glass where the translational density fluctuations are quasi-ergodic, except for very small wave vectors q . Within MCT, dynamic slowing down associated to a glass transition is driven by the amplitude of the static correlations. Since the approach of the nematic transition line is accompanied by an increase of the nematic order correlation function at $q = 0$, the non-linear feedback mechanism of MCT results in a glass transition, already before macroscopic nematic order occurs [10]. In the arrested state, rotational motions become hindered.

The recently evaluated random close packing line [13] for HE also exhibits a swallow-like shape. Although Kerr effect measurements in the isotropic phase of liquid crystals have given some evidence for the existence of two types of glass transitions [14] (related to nematic phase formation and to cage effect respectively) almost nothing is known about the glassy dynamics of system forming liquid crystals in general and for HE in particular.

We perform an extended study of the dynamics of monodisperse HE in a wide window of ϕ and X_0 values, extending the range of X_0 previously studied [15]. We specifically focus on establishing the trends leading to dynamic slowing down in both translations and rotations, by evaluating the loci of constant translational and rotational diffusion. These lines, in the limit of vanishing diffusivities, approach the glass-transition lines. We also study translational and rotational correlation functions, to search for the onset of slowing down and stretching in the decay of the correlation. We perform event-driven (ED) molecular dynamics simulations, using a new algorithm [16], which differently from previous algorithms [15, 17], relies on evaluations of distance between objects of arbitrary shape. We simulate a system of $N = 512$ ellipsoids at various volumes $V = L^3$ in a cubic box of edge L with periodic boundary conditions. We chose the geometric mean of the axis $l = \sqrt[3]{ab^2}$ as unit of distance, the mass m of the particle as unit of mass ($m = 1$) and $k_B T = 1$ (where k_B is the Boltzmann constant and T is the temperature) and hence the corresponding unit of time is $\sqrt{ml^2/k_B T}$. The inertia tensor is chosen as $I_x = I_y = 2mr^2/5$, where $r = \min\{a, b\}$. The value of the I_z component is irrelevant [18], since the angular velocity along the symmetry (z -) axis of the HE is conserved. We simulate a grid of more than 500 state points at different X_0 and ϕ as shown in Fig. 1. To create the starting configuration at a desired ϕ , we generate a random distribution of ellipsoids at very low ϕ and then we progressively decrease L up to the desired ϕ . We then equilibrate the configuration by propagating the trajectory for times such that both angular and translational correlation functions have decayed to zero. Finally, we perform a production run at least 30 times longer than the time needed to equilibrate. For the points close to the I-N transition we check the nematic order by evaluating the largest eigenvalue S of the order tensor \mathbf{Q} [19], whose components are:

$$Q_{\alpha\beta} = \frac{3}{2} \frac{1}{N} \sum_i \langle (\mathbf{u}_i)_\alpha (\mathbf{u}_i)_\beta \rangle - \frac{1}{3} \delta_{\alpha,\beta} \quad (1)$$

where $\alpha, \beta \in \{x, y, z\}$, and the unit vector $(\mathbf{u}_i(t))_\alpha$ is the component α of the orientation (i.e. the symmetry axis) of ellipsoid i at time t . The largest eigenvalue S is non-zero if the system

is nematic and 0 if it is isotropic. In the following, we choose the value $S = 0.3$ as criteria to separate isotropic from nematic states. From the grid of simulated state points we build

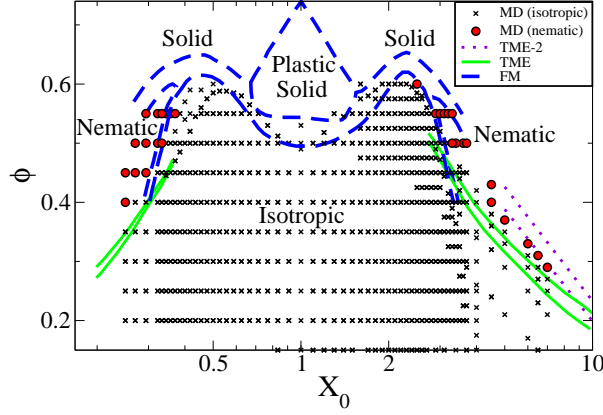


FIG. 1: Grid of state points simulated (crosses and red-filled circles) and relevant boundary lines of coexistence regions. Long-dashed curves are coexistence curves of all first order phase transitions in the phase diagram of HE evaluated by Frenkel and Mulder (FM)[9]. Solid lines are coexistence curves for the I-N transition of oblate and prolate ellipsoids, obtained analytically by Tijpto-Margo and Evans [6] (TME). Dotted lines (TME-2) are coexistence curves of prolate ellipsoids for the I-N transition, taken from [6].

a corresponding grid of translational (D_{trans}) and diffusional (D_{rot}) coefficients, defined as:

$$D_{trans} = \lim_{t \rightarrow +\infty} \frac{1}{N} \sum_i \frac{\langle \|\mathbf{x}_i(t) - \mathbf{x}_i(0)\|^2 \rangle}{6t} \quad (2)$$

$$D_{rot} = \lim_{t \rightarrow +\infty} \frac{1}{N} \sum_i \frac{\langle \|\Delta\Phi_i\|^2 \rangle}{4t} \quad (3)$$

where $\Delta\Phi_i = \int_0^t \omega_i dt$, \mathbf{x}_i is position of the center of mass and ω_i is the angular velocity of ellipsoid i . By proper interpolation, we evaluate the isodiffusivity lines, shown in Fig. 2. Results show a striking decoupling of the translational and rotational dynamics. While the translational isodiffusivity lines mimic the swallow-like shape of the coexistence between the isotropic liquid and the crystalline phases (as well as the MMCT prediction for the glass transition[10]), rotational isodiffusivity lines reproduce qualitatively the shape of the I-N coexistence. As a consequence of the the swallow-like shape, at large fixed ϕ , D_{trans} increases by increasing the particle's anisotropy, reaching its maximum at $X_0 \approx 0.5$ and

$X_0 \approx 2$. Further increase of the anisotropy results in a decrease of D_{trans} . For all X_0 , an increase of ϕ at constant X_0 leads to a significant suppression of D_{trans} , demonstrating that D_{trans} is controlled by packing. The iso-rotational lines are instead mostly controlled by X_0 , showing a progressive slowing down of the rotational dynamics independently from the translational behavior. This suggests that on moving along a path of constant D_{trans} , it is possible to progressively decrease the rotational dynamics, up to the point where rotational diffusion arrest and all rotational motions become hindered. Unfortunately, in the case of monodisperse HE, a nematic transition intervenes well before this point is reached. It is thus stimulating to think about the possibility of designing a system of hard particles in which the nematic transition is inhibited by a proper choice of the disorder in the particle's shape/elongations. We note that the slowing down of the rotational dynamics is consistent with MMCT predictions of a nematic glass for large X_0 HE[10], in which orientational degrees of freedom start to freeze approaching the isotropic-nematic transition line, while translational degrees of freedom mostly remain ergodic. To support the possibility that the slowing down of the dynamics on approaching the nematic phase originates from a close-by glass transition, we evaluate the self part of the intermediate scattering function F_{self}

$$F_{self}(q, t) = \frac{1}{N} \langle \sum_j e^{i\mathbf{q} \cdot (\mathbf{x}_j(t) - \mathbf{x}_j(0))} \rangle \quad (4)$$

and the second order orientational correlation function $C_2(t)$ defined as [15] $C_2(t) = \langle P_2(\cos \theta(t)) \rangle$, where $P_2(x) = (3x^2 - 1)/2$ and $\theta(t)$ is the angle between the symmetry axis at time t and at time 0. The $C_2(t)$ rotational isochrones are found to be very similar to rotational isodiffusivity lines.

These two correlation functions never show a clear two-step relaxation decay in the entire studied region, even where the isotropic phase is metastable, since the system can not be significantly over-compressed. As for the well known hard-sphere case, the amount of over-compressing achievable in a monodisperse system is rather limited. This notwithstanding, a comparison of the rotational and translational correlation functions reveals that the onset of dynamic slowing down and glassy dynamics can be detected by the appearance of stretching. Fig. 3 contrasts the shape of F_{self} , evaluated at $q = q_{max}$, where q_{max} is the q corresponding to the first maximum of the center-of-mass static structure factor, and $C_2(t)$ at $\phi = 0.50$ for different X_0 values with best-fit based on an exponential ($\sim \exp[-t/\tau]$) and a stretched exponential ($\sim \exp[-(t/\tau)^\beta]$) decay. As a criteria to avoid including in the fit the short-time

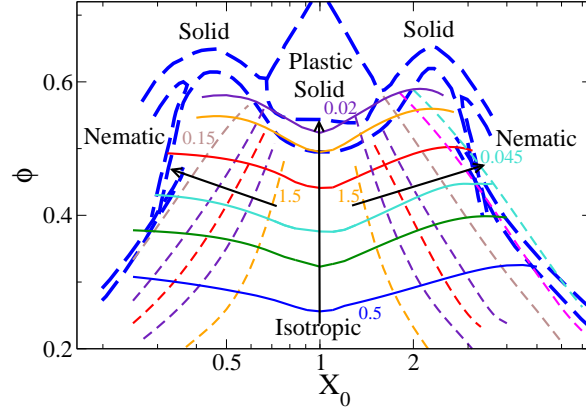


FIG. 2: Isodiffusivity lines. Solid lines are isodiffusivity lines from translational diffusion coefficients D_{trans} and dashed lines are isodiffusivities lines from rotational diffusion coefficients D_{rot} . Arrows indicate decreasing diffusivities. Left and right arrows refer to rotational diffusion coefficients. Diffusivities along left arrow are: 1.5, 0.75, 0.45, 0.3, 0.15. Diffusivities along right arrow are: 1.5, 0.75, 0.45, 0.3, 0.15, 0.075, 0.045. Central arrow refers to translational diffusion coefficients, whose values are: 0.5, 0.3, 0.2, 0.1, 0.04, 0.02. Thick long-dashed lines are FM and TME coexistence lines from Fig.1

ballistic contribution, we limit the time-window to times larger than t^* , defined for F_{self} and C_2 as the time at which the autocorrelation function of center-of-mass velocity \mathbf{v} ($\phi_{vv}(t) \equiv \frac{1}{N} \sum_i \langle \mathbf{v}_i(t) \mathbf{v}_i(0) \rangle$) and of angular velocity respectively ($\phi_{\omega\omega}(t) \equiv \frac{1}{N} \sum_i \langle \omega_i(t) \omega_i(0) \rangle$) reaches $1/e$ of its initial value. We note that F_{self} shows an exponential behaviour close to the I-N transition ($X_0 = 3.2, 0.3448$) on the prolate and oblate side, in agreement with the fact that translational isodiffusivities lines do not exhibit any peculiar behaviour close to the I-N line. Only when $X_0 \approx 1$, F_{self} develops a small stretching, consistent with the minimum of the swallow-like curve observed in the fluid-crystal line [20, 21], in the jamming locus as well as in the predicted behavior of the glass line for HE[10] and for small elongation dumbbells[22, 23]. Opposite behavior is seen for the case of the orientational correlators. C_2 shows stretching at large anisotropy, i.e. at small and large X_0 values, but decays within the microscopic time for almost spherical particles. In this quasi-spherical limit, the decay is well represented by the decay of a free rotator[24]. Previous studies of the rotational

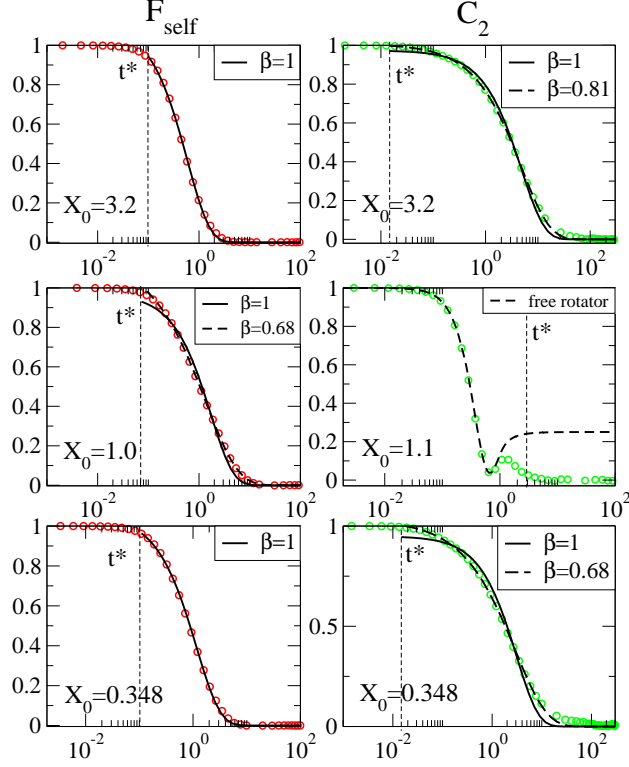


FIG. 3: Shape of F_{self} and C_2 at $\phi = 0.50$ for different X_0 . Symbols are data from MD simulations. Solid lines are fits to exponential functions, while long-dashed lines are fits to stretched exponentials (β is the stretching parameter). t^* is the time at which correlation functions ϕ_{vv} and $\phi_{\omega\omega}$, for F_{self} and C_2 respectively, reach $1/e$ of their initial values. Top: Prolate ellipsoids with $X_0 = 3.2$, C_2 shows a significant stretching while F_{self} decays exponentially. Center: $X_0 = 1.0$ for F_{self} and $X_0 = 1.1$ for C_2 , the dashed line is the theoretical decay of a free rotator C_2^f ($C_2^f(t) = 1 - \frac{3}{2} \frac{t}{\tau_f} \exp[-t^2/\tau_f^2] \tilde{\Phi}(t/\tau_f)$, where $\tau_f^2 = 1/\phi_{\omega\omega}(0)$ and $\tilde{\Phi}(t) = \int_0^t \exp[x^2] dx$). Bottom: Oblate ellipsoids with $X_0 = 0.348$.

dynamics of HE[15] did not report stretching in C_2 , probably due to the smaller values of X_0 previously investigated and to the present increased statistic which allows us to follow the full decay of the correlation functions.

Fig. 3 clearly shows that C_2 becomes stretched approaching the I-N transition while F_{self} remains exponential on approaching the transition. To quantify the amount of stretching in C_2 we show in Fig. 4 the X_0 dependence of τ and β for three different values of ϕ . In all cases, slowing down of the characteristic time and stretching increases progressively on approaching the I-N transition. It is interesting to observe that the amount of stretching

appears to be more pronounced in the case of oblate HE compared to prolate ones. A similar (slight) asymmetry between oblate and prolate HE can be observed in the lines reported in Figure 2.

In summary, we have shown that clear precursors of dynamic slowing down and stretching can be observed in the region of the phase diagram where a (meta)stable isotropic phase can be studied. Despite the monodisperse character of the present system prevents the possibility of observing a clear glassy dynamics, our data suggest that a slowing down in the orientation degree of freedom — driven by the elongation of the particles — is in action. The main effect of this shape-dependent slowing down is a decoupling of the translational and rotational dynamics which generates an almost perpendicular crossing of the D_{trans} and D_{rot} isodiffusivity lines. This behavior is in accordance with MMCT predictions, suggesting two glass transition mechanisms, related respectively to cage effect (active for $0.5 \lesssim X_0 \lesssim 2$) and to pre-nematic order ($X_0 \lesssim 0.5$, $X_0 \gtrsim 2$) [10]. It remains to be answered if it is possible to find a suitable model, for example polydisperse in size and elongation, for which nematization can be sufficiently destabilized, in analogy to the destabilization of crystallization induced by polydispersity in hard-spheres. We acknowledge support from MIUR-PRIN. We also

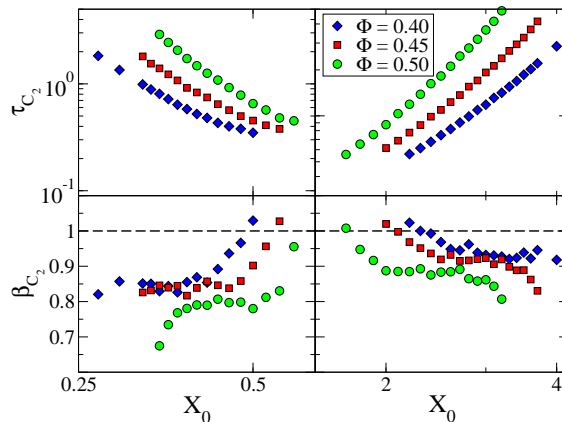


FIG. 4: β_{C_2} and τ_{C_2} are obtained from fits of C_2 to a stretched exponential for $\phi = 0.40, 0.45$ and 0.50 . Top: τ_{C_2} as a function of X_0 . Bottom: β_{C_2} as a function of X_0 . The time window used for the fits is chosen in such a way to exclude the microscopic short times ballistic relaxation (see text for details). For $0.588 < X_0 < 1.7$ the orientational relaxation is exponential.

thank A. Scala for suggesting code optimization and taking part to the very early stage of

this project.

-
- [1] M. P. Allen, in *Computational Soft Matter: From Synthetic Polymers to Proteins*, edited by N. Attig, K. Binder, H. Grubmüller, and K. Kremer (John von Neumann Institute for Computing, 2004), vol. 23, pp. 289–320.
 - [2] L. Onsager, *Ann. N. Y. Acad. Sci.* **51**, 627 (1949).
 - [3] J. D. Parsons, *Phys. Rev. A* **19**, 1225 (1979).
 - [4] S.-D. Lee, *J. Chem. Phys.* **89**, 7036 (1989).
 - [5] A. Samborski, G. T. Evans, C. P. Mason, and M. P. Allen, *Mol. Phys.* **81**, 263 (1994).
 - [6] B. Tjijto-Margo and G. T. Evans, *J. Chem. Phys.* **93**, 4254 (1990).
 - [7] W. Götze, in *Liquids, Freezing and the Glass Transition*, edited by J. P. Hansen, D. Levesque, and J. Zinn-Justin (North-Holland, 1991).
 - [8] G. S. Singh and B. Kumar, *Ann. Phys.* **24**, 294 (2001).
 - [9] D. Frenkel and B. M. Mulder, *Molec. Phys.* **55**, 1171 (1991).
 - [10] M. Letz, R. Schilling, and A. Latz, *Phys. Rev. E* **62**, 5173 (2000).
 - [11] T. Franosch, M. Fuchs, W. Götze, M. R. Mayr, and A. P. Singh, *Phys. Rev. E* **56**, 5659 (1997).
 - [12] R. Schilling and T. Scheidsteger, *Phys. Rev. E* **56**, 2932 (1997).
 - [13] A. Donev, I. Cisse, D. Sachs, E. A. Variano, F. H. Stillinger, R. Connelly, S. Torquato, and P. M. Chaikin, *Science* **303**, 990 (2004).
 - [14] H. Cang, J. Li, V. N. Novikov, and M. D. Fayer, *J. Chem. Phys.* **118**, 9303 (2003).
 - [15] M. P. Allen and D. Frenkel, *Phys. Rev. Lett.* **58**, 1748 (1987).
 - [16] C. De Michele and A. Scala, in preparation.
 - [17] A. Donev, F. H. Stillinger, and S. Torquato, *J. Comp. Phys.* **202**, 737 (2005).
 - [18] M. P. Allen, D. Frenkel, and J. Talbot, *Molecular Dynamics Simulations Using Hard Particles* (North-Holland, 1989).
 - [19] S. C. McGrother, D. C. Williamson, and G. Jackson, *J. Chem. Phys.* **104**, 6755 (1996).
 - [20] P. N. Pusey and W. van Megen, *Phys. Rev. Lett.* **59**, 2083 (1987).
 - [21] W. G. Hoover and F. H. Ree, *J. Chem. Phys.* **49**, 3609 (1968).
 - [22] S.-H. Chong, A. J. Moreno, F. Sciortino, and W. Kob, *Phys. Rev. Lett.* **94**, 215701 (2005).
 - [23] S.-H. Chong and W. Götze, *Phys. Rev. E* **65**, 041503 (2002).

[24] C. Renner, H. Löwen, and J. L. Barrat, Phys. Rev. E **52**, 5091 (1995).